Time-Resolved Light Scattering Studies on the Early Stage of Crystallization in Poly(ethylene terephthalate)

Chang Hyung Lee, Hiromu Saito, and Takashi Inoue*

Department of Organic and Polymeric Materials, Tokyo Institute of Technology, Ookayama, Meguro-ku, Tokyo 152, Japan

Received May 18, 1993; Revised Manuscript Received September 1, 1993®

ABSTRACT: Crystallization kinetics in poly(ethylene terephthalate) (PET) was investigated by time-resolved light scattering under H_v (cross-polarized) and V_v (parallel-polarized) optical alignments using a highly sensitive CCD (charge-coupled device) camera system. When the background intensity was subtracted from the observed two-dimensional CCD image, only the four-leaf-clover pattern was obtained even at the early stage of crystallization. This suggests that the spherulites are generated at an early stage and grow without change of shape. Previously, from photographic light scattering results, it was believed that the evolution of PET spherulites proceeded from rodlike and sheaflike crystallites. The relative degree of crystallinity given by the invariant method and the disorder parameter defined by the angular dependence of scattered intensity revealed the formation of the isotropic embryo which is a highly disordered crystalline domain with low crystallinity. It grows up to yield the spherulite by increasing the size and the degree of ordering.

Introduction

A spherulite is a crystal aggregate with spherical symmetry. Such aggregation arises by radial growth of crystal from a common center. The spherulitic growth is believed to occur in two ways.[1,2] In the growth mechanism A, a central nucleating entity initiates crystal growth in all directions. In the growth mechanism B, the spherulite develops from one single crystal through essentially unidirectional growth and the spherical shape is attained through continuous branching and fanning via the intermediate stage of sheaves.[2]

The above schemes have come mostly from microscopic observations by polarized microscopy and transmission electron microscopy (TEM). Polarized microscopy is usually informative on the morphology from a few microns to several tens of microns. TEM provides the morphology on different levels of the structural hierarchy, i.e., from the lamellar level to the spherulitic architecture. However, for the TEM observation, one has to cool the specimen crystallized at high crystallization temperature (T_c) down to room temperature to carry out the pretreatment, such as the permanganic etching and the RuO_4 staining. If some structural change takes place after the drop from T_c to room temperature, the TEM information does not describe the morphology developed at T_c. Real-time observation at T_c is desirable to discuss the kinetics of spherulite growth.

By the photographic light scattering studies on the quenched specimen, Stein and Misra[3] concluded that the evolution of poly(ethylene terephthalate) (PET) spherulites proceeds by mechanism B; i.e., initially a rodlike structure forms which then evolves into sheaves and finally into spheres. We recently observed a completely different crystallization mechanism in isotactic polypropylene.[4] It motivated a real-time investigation of a morphology development of PET at T_c. In this paper, we carry out time-resolved light scattering studies by using a highly sensitive (charge-coupled device) (CCD) camera system.

Experimental Section

PET was supplied by Toyobo Co., Ltd. ($M_w = 6 \times 10^3$, $M_n = 3 \times 10^3$). PET pellets were dried under vacuum (10^{-4} mmHg) at 160 °C for 16 h to remove water completely. A thin-layer specimen (ca. 30 μm thick) was prepared by pressing the pellets between two cover glasses at 310 °C for 3 min and then was quenched in a liquid-nitrogen bath to obtain the glassy amorphous specimen.

The melt-quenched amorphous specimen was inserted into a light scattering hot stage set at a desired crystallization temperature T_c. A polarized He–Ne gas laser of 632.8-nm wavelength was applied vertically to the film specimen. The scattered light passed through an analyzer and then onto a highly sensitive CCD camera with 576 × 382 pixels in a sensor of dimensions 13.3 × 8.8 mm (Princeton Instruments, Inc.). This realizes the time-resolved measurement of a two-dimensional angular distribution of scattered light with 576 × 382 data points in a time scale of 10 s and that of a one-dimensional one with 576 data points in a time scale of 0.14 s. The input data from the CCD camera was digitized by the ST-13X controller. The digitized data were stored in a personal computer for further analysis. We also employed the classic photographic technique[3,5] to observe the scattering patterns. We employed two optical geometries; one was the H_v geometry in which the optical axis of the analyzer was set perpendicularly to that of the polarizer, and the other was the V_v geometry with a parallel set of the two axes.

Results and Discussion

The change of the H_v light scattering patterns during the isothermal crystallization at 120 °C are shown in Figure 1. The observed scattering patterns, obtained by the photographic method, exhibit the change from rodlike (a′) to racquet (b′) and then to a four-leaf-clover type (c′) with crystallization time. That is, the result by Stein and Misra[3] is reproduced here. Comparing the observed patterns with theoretical ones, such change suggests a rodlike aggregate forms initially which then evolves into sheaves and finally into spherulites. However, when the background intensity was subtracted from the observed two-dimensional CCD image, rodlike and racquet patterns disappeared and only the four-leaf-clover pattern characteristic of spherulites was obtained as shown in Figure 1a–c.[5] The clover pattern became smaller with time of crystallization from a to c in Figure 1. The results suggest that the spherulite is formed even at the early stages of crystallization and then grows with time without changing shape.

Figure 2 shows the one-dimensional H_v scattering profiles at an azimuthal angle 45° in the scattering patterns at various crystallization times. The profile has a maximum at a scattering angle θ_m. This is a hallmark of a four-leaf-clover pattern in parts a–c of Figure 1. One can

* To whom correspondence should be addressed.

® Abstract published in *Advance ACS Abstracts*, October 15, 1993.

0024-9297/93/2226-6566$04.00/0

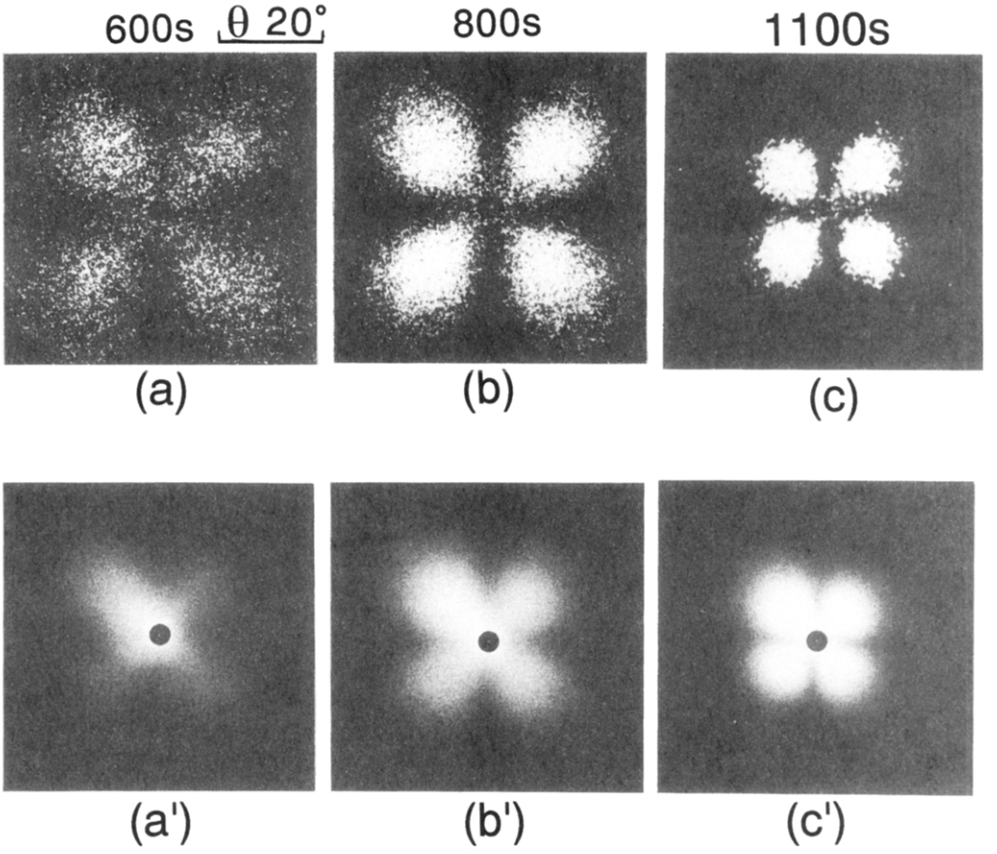

Figure 1. Series of H_v light scattering patterns during the crystallization at T_c = 120 °C: (a–c) obtained by a CCD camera, subtracting the background intensity from the observed one; (a′–b′) obtained by the photographic method.

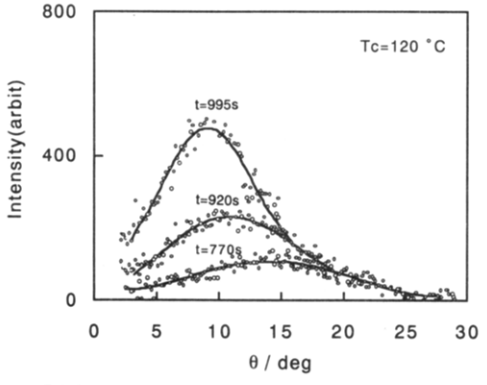

Figure 2. Light scattering profiles for various crystallization times.

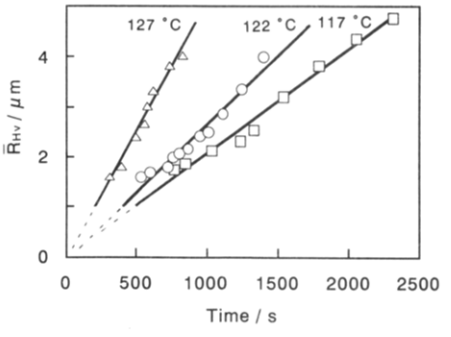

Figure 3. Time variation of the radius of the spherulite.

obtain the average radius of spherulites $\bar{R}_{H_v}$ by the θ_m:[6]

$$4.09 = 4\pi(\bar{R}_{H_v}/\lambda)\sin(\theta_m/2) \quad (1)$$

Time variation of the radius of the spherulite $\bar{R}_{H_v}$ at various crystallization temperatures T_c is shown in Figure 3. A linear growth of the spherulite is seen. An extrapolation of the linear growth region to zero radius leads to a positive or nearly zero intercept of the time. That is, the positive or zero induction time is obtained. This result is different from that of Stein and Misra,[3] in which negative induction times were found, suggesting that the structure is not spherulitic at early stages of the crystallization.

Assuming that the number of spherulites is constant and no impingement occurs during the crystallization, the crystallinity ϕ_s is given by

$$\phi_s = (\bar{R}_{H_v}/R_m)^3 \quad (2)$$

where $\bar{R}_m$ is the maximum radius of the spherulite, i.e., the attainable radius before the impingement. When the Avrami equation[7] is applied for the early stage, the time variation of ϕ_s is given by

$$\phi_s = 1 - \exp[-\beta(t - t_0)^\alpha] \quad (3)$$

where α is the Avrami index, which depends on the mode of crystal growth or the shape of the crystallites, and β is the overall crystallization rate constant. Avrami plots at the early stage of crystallization for various crystallization temperatures are shown in Figure 4. The plots yield straight lines, indicating that α does not change with time. The constant $\alpha \approx 3$ suggests the heterogeneous nucleation and three-dimensional crystal growth. The constant α may be ascribed to the fixed crystallite structure with time. This supports the results in parts a–c of Figure 1; i.e., the spherulite exists even at early stages and grows up without the change of its shape during the crystallization. That is, the shape of the crystallites does not change with time. For a deeper understanding of such a spherulitic growth, we extend the discussion in the early stage of the crystallization in more detail as follows.

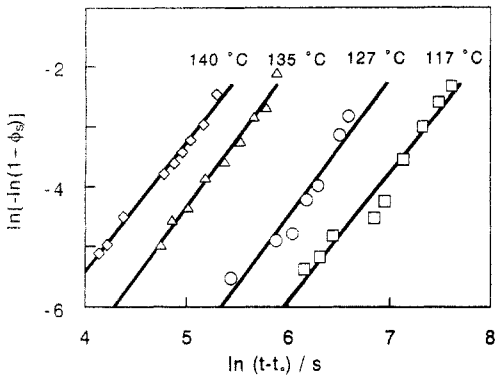

Figure 4. Avrami plots.

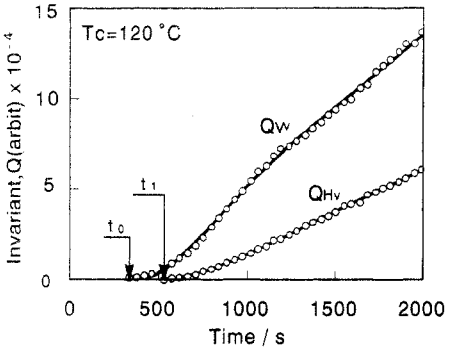

Figure 5. Time variations of the invariants Q_{H_v} and Q_{V_v}.

To discuss the crystallization kinetics, it is convenient to employ the integrated scattering intensity, i.e., the invariant Q defined by[8]

$$Q = \int_0^\infty I(q) q^2 \, dq \tag{4}$$

where q is the scattering vector, $q = (4\pi/\lambda)\sin(\theta/2)$, λ and θ being the wavelength and scattering angle, respectively, and $I(q)$ is the intensity of the scattered light at q.

The H_v scattering pattern from the crystallized specimen was a four-leaf-clover type. In this case, the invariant, Q_{H_v}, is described by the mean-square optical anisotropy $\langle \delta^2 \rangle$

$$Q_{H_v} \propto \langle \delta^2 \rangle = \phi_s \delta_s^{\,2} \tag{5}$$

$$\delta_s = \phi_{sc}(\alpha_1 - \alpha_2) \tag{6}$$

where ϕ_{sc} is the internal crystallinity of the crystalline domain, and α_1 and α_2 are the principal polarizabilities of the crystal lamella.

On the other hand, the invariant in the V_v mode, Q_{V_v}, is ascribed to both $\langle \delta^2 \rangle$ and the mean-square density fluctuation $\langle \eta^2 \rangle$. The $\langle \eta^2 \rangle$ is given by

$$\langle \eta^2 \rangle = \phi_s(1 - \phi_s)(\alpha_s - \alpha_0)^2 \tag{7}$$

where α_s is the polarizability of the crystalline domain and α_0 is the polarizability of the melt.

The time variations of the invariants Q_{H_v} and Q_{V_v} at T_c = 120 °C are shown in Figure 5. Both invariants increase with the time of crystallization. However, the onset time is different. That is, $\langle \eta^2 \rangle$ starts to increase at $t = t_0$, and then after a certain time lag, the onset of $\langle \delta^2 \rangle$ is seen at $t = t_1$. In contrast, by the current understanding of spherulite growth, one may expect a simultaneous onset of $\langle \eta^2 \rangle$ and $\langle \delta^2 \rangle$. The question is, what happens during the time lag of $t_1 - t_0$.

The time lag may be ascribed to the development of an isotropic embryo as the precursor of the spherulite. However, what is the isotropic embryo? One may mention

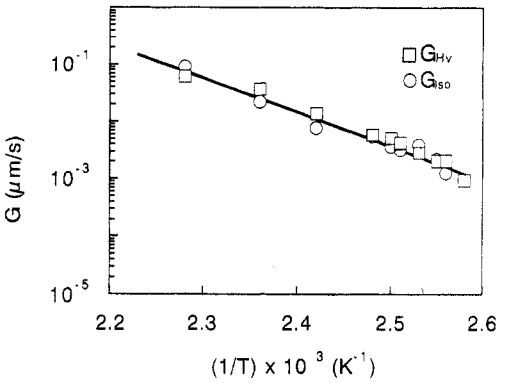

Figure 6. Temperature dependence of the growth rate of the isotropic domain and that of the spherulite.

two possibilities: one is a high-density domain by the thermal fluctuation, and the other is a less-ordered crystalline domain. If the former is the case, $\langle \eta^2 \rangle$ and $\langle \delta^2 \rangle$ will show an abrupt increase when the high-density domain transformed to the crystalline domain, say, at $t = t_1$. The result in Figure 5 is against this; i.e., $\langle \eta^2 \rangle$ and $\langle \delta^2 \rangle$ increase continuously with time at the early stage. The latter possibility seems to be more realistic. It implies that one has to discuss the crystallization kinetics by taking account of the isotropic nature in the early stages.

The V_v scattering patterns up to $t = t_1$ were of the circular-symmetric type; i.e., there was no azimuthal angular dependence. The angular dependence at the time window $t_1 - t_0$ was well described by the Debye–Bueche type scattering function[9,10]

$$I(q) = \left(\frac{1}{A + Bq^2}\right)^2 \tag{8}$$

where A and B are constants. If the isotropic embryo is spherical, its average radius $\bar{R}_{iso}$ is given as a function of the Debye–Bueche correlation distance $a = (B/A)^{1/2}$ (see eq 8) and the volume fraction ϕ_s:

$$\bar{R}_{iso} = \frac{3a}{4(1 - \phi_s)} \tag{9}$$

Here, since t_1 is much shorter than the half-crystallization time, in which the Q_{V_v} attains a maximum, we may assume $\phi_s = 0$. The time variation of the radius of the isotropic domain $\bar{R}_{iso}$ showed a linear growth of the isotropic embryo. From the slope, the growth rate G_{iso} ($=d\bar{R}_{iso}/dt$) was obtained.

The temperature dependence of G_{iso} is shown by the open circles in Figure 6. Here also shown by open squares are the growth rate of spherulites G_{H_v} obtained by the slope in Figure 3. Both temperature dependences of G_{iso} and G_{H_v} are similar. This suggests that the isotropic embryo has the crystalline nature; i.e., the isotropic embryo may be the less-ordered crystalline domain, and its growth is governed by the crystallization kinetics. Now, following the above scenario, the isotropic embryo exists at the early stage, and then it would grow up to the more-ordered domain, such as the spherulite. The discussion of kinetics should be extended to the intermediate and late stages.

Using eqs 3, 5, and 6, a relative degree of crystallinity in the crystalline domain Φ_{cs} may be described by

$$\Phi_{cs} = \frac{\phi_{sc}(t)}{\phi_{sc}(\infty)} = \frac{\langle \delta^2 \rangle_t^{1/2}}{\langle \delta^2 \rangle_\infty^{1/2} [\phi_s]^{1/2}} \tag{10}$$

where $\phi_{sc}(\infty)$ is the attainable crystallinity in the crystalline domain (i.e., impinged spherulite) at a given crystallization condition. Typical time variations of Φ_{cs} estimated by eq

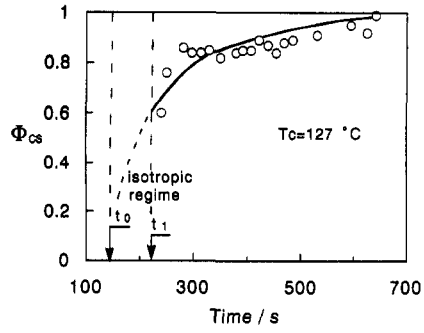

Figure 7. Time variation of the relative crystallinity Φ_{cs}.

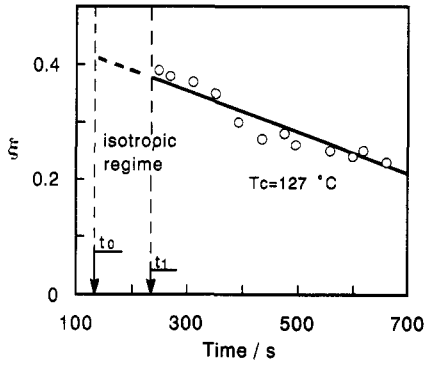

Figure 8. Time variation of disorder parameter ξ.

10 are shown in Figure 7. Φ_{cs} is found to increase gradually with time. That is, the crystallization proceeds in the domain with its growth. The extrapolated values of Φ_{cs} in the isotropic domain are small, suggesting a low crystallinity.

Thus the relative crystallinity seems to increase with time at the intermediate and late stages. Then the next problem to be discussed is the ordering process. The ordering can be analyzed in terms of scattering variables as follows.

According to Yoon and Stein,[11] the disorder parameter ξ is described by the orientation-angle fluctuation of the optic axis within a spherulite. They suggested by the model calculation of the scattering patterns that the large ξ results in the broad H_v scattering profile; i.e., as ξ increases, the intensity at θ_m decreases and the intensity decreases more gradually with θ. They provided a calibration curve relating the parameter ξ to the ratio of the intensity at $w = 4$ to that at $w = 15$, where w is the reduced angle parameter defined by $(2\pi/\lambda)\bar{R}_{H_v} \sin\theta$ (see Figure 7 of ref 11).

Using the calibration curve, the values of ξ were calculated from the scattering profiles in Figure 2. The results are shown in Figure 8. The disorder parameter is shown to decrease with time. If one extrapolates the results in Figure 8 to the early stage, at which the H_v scattering has not been detected and hence ξ cannot be defined, the ξ values are expected to be very large. It implies that the crystalline arrangement is highly disordered in the isotropic domain. Further, recalling the similar argument in Figure 7 that the crystallinity Φ_{cs} should be very low at the early stage, one may conclude that the isotropic domain is a crystalline one with low Φ_{cs} and high ξ. The disordered domain with a low crystallinity should look isotropic for the light so that it will render the time lag in Figure 5.

ξ versus spherulite radius $\bar{R}_{H_v}$ is plotted at various temperatures in Figure 9. ξ decreases more steeply with

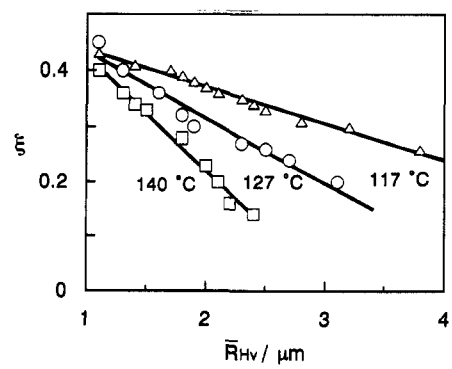

Figure 9. Plot of ξ versus $\bar{R}_{H_v}$ at various temperatures.

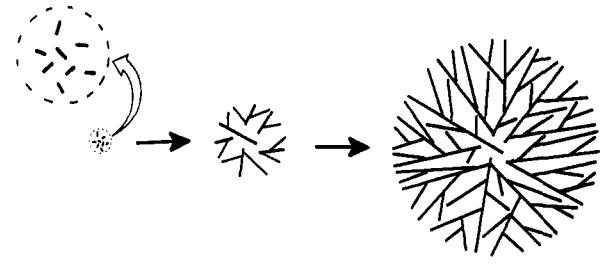

Figure 10. Schematic diagrams for the evolution of PET spherulite.

increasing temperature. This suggests that the rate for ordering increases with increasing temperature.

Conclusion

It had been shown by real-time small-angle light scattering studies on PET at the crystallization temperature that the previously held idea that the spherulitic morphology evolves from growth habits about a sheaflike nucleus could not describe the observations. The scattering analysis revealed that, at the early stage of crystallization, highly disordered crystalline domains with low crystallinity appear and, by increasing the size and the degree of ordering, they develop to yield the spherulite, as schematically depicted in Figure 10.

Acknowledgment. We are grateful to Masami Okamoto, Toyobo Co., Ltd., for a supply of the PET sample and interesting discussion.

References and Notes

(1) Wunderlich, B. *Macromolecular Physics*; Academic Press: New York, 1973; Chapter 3.7.
(2) Norton, B. R.; Keller, A. *Polymer* **1985**, *26*, 704.
(3) Misra, A.; Stein, R. S. *J. Polym. Sci., B* **1972**, *10*, 473.
(4) Okada, T.; Saito, H.; Inoue, T. *Macromolecules* **1992**, *25*, 1908.
(5) The diffuse and weak background scattering appeared in the small scattering angle region in the H_v geometry. This may arise from stray light due to the incomplete depolarization of the geometry. It is usually weak but comparable to the very weak H_v scattering at the early stages of crystallization. Consequently, the combined pattern of the background scattering with the weak four-leaf-clover pattern results in the rodlike or racquet pattern shown in parts a′ or b′ of Figure 1.
(6) Stein, R. S.; Rhodes, M. B. *J. Appl. Phys.* **1960**, *31*, 1873.
(7) Avrami, M. J. *J. Chem. Phys.* **1939**, *7*, 1103.
(8) Koberstein, T.; Russell, T. P.; Stein, R. S. *J. Polym. Sci., Polym. Phys. Ed.* **1979**, *17*, 1719.
(9) Debye, P.; Bueche, A. M. *J. Appl. Phys.* **1949**, *20*, 518.
(10) Debye, P.; Anderson, H. R.; Brumberger, H. J. *J. Appl. Phys.* **1957**, *28*, 679.
(11) Yoon, D. Y.; Stein, R. S. *J. Polym. Sci., Polym. Phys. Ed.* **1974**, *12*, 763.